JBC Papers in Press. Published on September 28, 2009 as Manuscript M109.043737
The latest version is at http://www.jbc.org/cgi/doi/10.1074/jbc.M109.043737

# FAST DIFFUSION OF VERY LONG CHAIN SATURATED FATTY ACIDS ACROSS A BILAYER MEMBRANE AND THEIR RAPID EXTRACTION BY CYCLODEXTRINS: IMPLICATIONS FOR ADRENOLEUKODYSTROPHY*

**Biju K. Pillai[1], Ravi Jasuja[2], Jeffrey R. Simard[1,3,§] and James A. Hamilton[1,4]**
From the Department of Biophysics and Physiology[1], Section of Endocrinology, Diabetes and Nutrition[2], Department of Pharmacology & Experimental Therapeutics[3] at Boston University School of Medicine, Boston, Massachusetts 02118
From the Department of Biomedical Engineering[4] at Boston University, Boston, Massachusetts 02118
[§] Current address: Chemical Genomics Centre of the Max-Planck-Society, Otto-Hahn-Strasse 15, D-44227 Dortmund, Germany
Running head: Very long chain fatty acids and adrenoleukodystrophy
Address correspondence to: James A. Hamilton, Ph.D., Boston University School of Medicine, 715 Albany St., Boston, MA 02118. Tel: +1-617-638-5048; E-mail: jhamilt@bu.edu

**Abnormalities in the transport of saturated very long chain fatty acids (VLCFA; > C18:0) contribute to their toxic levels in peroxisomal disorders of fatty acid (FA) metabolism, such as adrenoleukodystrophy (ALD) and adrenomyeloneuropathy (AMN). We previously showed that VLCFA desorb much slower than normal dietary FA from both albumin and protein-free lipid bilayers. The important step of transbilayer movement (flip-flop) was not measured directly as a consequence of this very slow desorption from donors, and the extremely low aqueous solubility of VLCFA precludes addition of unbound VLCFA to lipid membranes. We have overcome these limitations using methyl-β-cyclodextrin (MβCD) to solubilize VLCFA for rapid delivery to 'acceptor' phosphatidylcholine (PC) vesicles (small and large unilamellar) and to cells. VLCFA binding was monitored in real time with the fluorescent probe FPE in the outer membrane leaflet, while entrapped pyranine was used to detect flip-flop across the membrane. The upper limit of the rate of flip-flop across the membrane was independent of temperature, media viscosity and was similar for model raft and non-raft membranes as well as in living cells. We further showed that cyclodextrins can extract VLCFA rapidly (within sec) from vesicles and cells which have implications for the mechanism and potential alternative approaches to treat ALD. Since VLCFA diffuse through the lipid bilayer, proteins may not be required for their transport across the peroxisomal membrane.**

Elevated levels of saturated very long-chain saturated fatty acids (VLCFA; > 18 carbons) in plasma serve as a biomarker for certain inherited neurological disorders includng adrenoleukodystrophy (ALD) (1) (2-4). Several peroxisomal biogenesis disorders (Zellweger syndrome, neonatal ALD, and infantile Refsum disease) and deficiencies of peroxisomal fatty acid (FA) degradation enzymes are also marked by abnormally high levels of VLCFA (5,6). However, the clinical manifestations are quite different (1,7) and it is not clear whether there is a common underlying biophysical or biochemical mechanism. It is generally presumed that VLCFA accumulate mainly because of inefficient degradation (β-oxidation), which normally takes place in the peroxisomes (8-11), or possibly because of the combination of impaired β-oxidation and enhanced FA elongation (12).

ALD patients are also known to have a mutation in the *abcd1* gene which encodes ALD protein (ALDP), an integral peroxisomal

membrane protein and a member of the ATP binding cassette transporter super family (13). *Abcd1*-knockout mice show VLCFA accumulation in brain tissue and have a neurological phenotype. Overexpression of ALDP in fibroblasts from both ALD patients and *abcd1*-knockout mice can reverse biochemical abnormalities (14). Elucidating the function of ALDP is critical to our understanding of the biochemical abnormalities in ALD. Transfection of fibroblasts from ALD patients with ALDP results in normal expression levels and partially corrects for defective VLCFA β-oxidation. A direct role has also been proposed in which ALDP actively transports acyl-CoAs across the peroxisomal membrane (11,15). Disregulation of such a mechanism would impair VLCFA metabolism and might also explain the accumulation of VLCFA in membranes.

The membrane transport of long-chain FA (≤ 18 carbons) has been investigated extensively in model and biological membranes (16-21). However, knowledge of the mechanisms of VLCFA transport are lacking. VLCFA have very low aqueous solubility, a property which limits its transport between aqueous compartments and is a major impediment to its study even in model membrane systems. VLCFA have been shown to exhibit very slow dissociation rates from both serum albumin and membranes into the surrounding aqueous phase (several orders of magnitude slower than that of typical dietary long-chain FA) (22) (23). Additionally, serum albumin has a much lower capacity for VLCFA. The very slow transfer of VLCFA between albumin and the plasma membrane led us to hypothesize that VLCFA are not simply markers of disease but could also act as pathogenic agents. Elevated levels of VLCFA in membranes could alter membrane structure and function (24). To understand more completely the role(s) VLCFA have in ALD, it is necessary to determine how rapidly they traverse the lipid bilayer membrane and whether or not a protein is required to actively facilitate this process.

Here we report that complexion of VLCFA with methyl-β-cyclodextrin (MβCD) eliminated slower kinetic steps, resulted in faster delivery of VLCFA to the membrane surface, and allowed direct investigation of whether VLCFA diffusion across both model and biological membranes is a slow process which would require catalysis by a protein such as ALDP. We report the first direct measure of VLCFA transmembrane movement. We not only demonstrated the fast flip-flop of VLCFA but also the fast removal of VLCFA from membranes by MβCD. In our assays with model membranes, we found that the rate of flip-flop was independent of temperature, indicating a minimal activation energy barrier associated with this process in protein-free model membranes.

## Experimental Procedures

*Chemicals.* Arachidic acid (C20:0), behenic acid (C22:0),) and hexacosanoic acid (C26:0), methyl-β-cyclodextrin (MβCD) and 2-hydroxypropyl-β-cyclodextrin (HPβCD) were purchased from Sigma (St. Louis, MO). HEPES was purchased from Aldrich Chemical Co. (Milwaukee, WI). Phosphatidylcholine isolated from chicken egg (PC), sphingomyelin and cholesterol were obtained from Avanti Polar Lipids, Inc. (Alabaster, AL). Sephadex G-25 was obtained from Pharmacia Biotech (Piscataway, NJ). Hydroxypyrene trisulfonic acid trisodium salt (pyranine) was purchased from Eastman Kodak Co. (Rochester, NY). Fluorescein-labeled phosphatidylethanolamine (FPE or DHPE), BCECF-AM and Prodan were obtained from Invitrogen/Molecular Probes (Carlsbad, CA).

*Stock Solutions.* The pyranine stock solution (10 mM) was prepared by dissolving pyranine in deionized water. The FPE stock (2.15 mg/ml) was prepared by dissolving lyophilized FPE in a 5:1 (v/v) mixture of $CHCl_3$:methanol as

described previously (20). VLCFA (C20:0) was dissolved in DMSO or ethanol to prepare 5 mM stock solutions. Prodan stock solution (2 mM) was prepared in DMSO.

*Preparation of Lipid Vesicles.* Small unilamellar vesicles (SUV) were prepared as described previously (20). In the case of model lipid raft SUV, PC, sphingomyelin and cholesterol were mixed in a 1:1:1 molar ratio using the same methods described for 100% PC vesicles. Large unilamellar vesicles (LUV) composed of egg PC were prepared by the extrusion method as described previously that produces unilamellar vesicles with ~1000 Å diameter (17). The pyranine (0.2 mM) and buffer concentrations (20 mM) for both types of vesicles were the same. Untrapped pyranine was removed by washing the vesicle prep through a gel filtration column (G-25 Sephadex) with 20 mM Hepes/KOH buffer (25). For VLCFA binding studies, the external leaflet of the pre-formed SUV and LUV were labeled with FPE (1 mole% relative to PC) as described previously (20). FPE is sensitive to the binding of charged FA anions at the outer membrane leaflet (20,26,27) and entrapped pyranine reports intravesicular pH changes induced by the diffusion of FA across the membrane (17,19,20).

*Preparation of VLCFA/Vesicle and VLCFA/MβCD Complexes.* For VLCFA/SUV complexes, the dried vesicle lipids were co-sonicated with VLCFA (C20:0, C22:0) to make "donor vesicles" as described previously (20). VLCFA (C20:0, C26:0) was complexed with methyl-β-cyclodextrin (MβCD) to improve solubility and increase the rate of delivery of VLCFA to the membrane surface. An MβCD stock (50 mM) was first prepared by dissolving the MβCD in deionized water. Different MβCD:VLCFA ratios were then used to dissolve ~2 mg of VLCFA (9:1 for C20:0 and 15:1 for C26:0) in water. The VLCFA/MβCD complex was then placed in a hot water bath (70-80$^{o}$C) for 2-3 min, vortexed intermittently and then pulse sonicated for 2-3 min to prepare a solution that was non-turbid at room temperature. All stock solutions were stored until use at -20$^{0}$C. Prior to fluorescence measurements, all VLCFA/MβCD solutions were brought to room temperature and vortexed before adding to a suspension of lipid vesicles containing pyranine or labeled with FPE.

*Fluorescence instrumentation real-time measurements with vesicles.* The fluorescence emission intensities of pyranine, FPE and Prodan were measured on a Spex® Fluoromax-2 (Jobin Yvon; Edison, NJ) and or using a K2 spectrofluorometer modified with data acquisition electronics and software from ISS (Champaign, IL). Emission intensity of FPE and pyranine were monitored prior to the addition of VLCFA to a rapidly stirred cuvette. The sample compartment of the fluorometer was temperature-regulated by an external water bath (25$^{o}$C), which delivered a continuous flow of water to a small metal plate located beneath the cuvette. .

Steady-state fluorescence measurements of FA binding and/or transmembrane movement in vesicles were performed by first preparing a suspension of acceptor vesicles (100 μM) in a cuvette containing 3 mL of 20 mM Hepes buffer (pH 7.4). The desired concentration of FA (complexed or uncomplexed) was delivered into the vesicle suspension through the injection port above the cuvette while continuously stirring using a mini stir bar. Under these conditions, the addition of the equivalent of 0.8, 1.5 and 3 μM VLCFA (see Supporting Information, Fig. S1b) correlates with the addition of 0.8, 1.5 and 3 mole% VLCFA with respect to PC. In vesicle-to-vesicle transfer studies of C20:0 and C22:0, the donor and acceptor vesicles were present in a 1:1 ratio in the final mixture. The fluorescence of pyranine and FPE were measured over time using a bandwidth of 3 nm and 3 nm for excitation and emission, respectively, for both probes. Pyranine was excited at 455 nm and emission measured at 509 nm; FPE was excited at 490 nm and emission was measured at 520 nm. The observed fluorescence change upon addition of different chain length FA from donor

vesicle, MβCD complex or without a carrier were further analyzed to determine the kinetics of the FA binding or transmembrane movement. Emission intensity of pyranine was monitored to study the chain length dependence of VLCFA (C20:0 and C26:0) extraction from the membrane by adding FA-free MβCD or hydroxypropyl β-cyclodextrin (HPβCD) at different concentrations.

To investigate the physical properties of phospholipid membranes, steady-state measurements of Prodan intensity were achieved by adding Prodan (3 μM) to a suspension SUV and measuring its emission spectra (over a range of 360 to 610 nm) approximately 3 min after adding the probe (probe/lipid ratio, 1:500) and exciting the sample at 359 nm (28-30)

*Kinetic Analysis.* The observed rate constant ($k_{obs}$) of the fluorescence change was obtained using the Origin software to fit each fluorescence trace to a first order decay function: $F(t) = F(t_\infty) + F(t_0)exp(-t*k_{obs})$, where $t$ is time, $F(t_0)$ is the initial fluorescence intensity, $F(t_\infty)$ is the fluorescence at $t = \infty$. The rate constant is related to the half-time of fluorescence change ($t_{1/2}$) by the equation: $t_{1/2} = ln\ 2 / k_{obs}$. All kinetic experiments were repeated 3-5 times.

*Preparation of cultured HEK-293 cells, cell imaging and real-time fluorescence measurements of cells.* HEK cells were cultured as described previously (31,32). Cell viability was checked by standard light microscopy. Labeling of cells with FPE was accomplished by first drying FPE and resuspending it in an equal volume of DMSO. Approximately 4 μl of FPE stock were added to the culture medium over cells attached to coverslips and gently agitated for 40 min in the dark at 37°C. For pH studies, cells were incubated for 40 min with the cell-permeable pH probe BCECF-AM and, prior to imaging, cells were washed three times with buffer (20 mM MOPS-KRB, pH 7.4) to remove any remaining probe in the media. BCECF was excited at 480 nm and the green fluorescence from BCECF was detected (PMT). Following addition of μM concentrations of C26:0/MβCD complex, cells were visualized under a 40X objective (oil immersion) and images were captured at different time intervals using a pixel size of 1024 x 1024 with an image acquisition time ~10 sec. All images were pseudo-colored using Image J (Wayne Rasband, NIH).

Real-time fluorescence measurements were made using similar protocols as those described above for vesicles. Cells (~$10^6$ cells) containing entrapped BCECF were suspended in buffer and then rapidly stirred in a cuvette. BCECF was monitored as a ratio of excitation wavelengths (R = 505 nm/ 435 nm) as C26:0/MCD complex was added directly into the cuvette through the injection port of the fluorimeter and when excess FA-free MβCD was added to extract VLCFA.

## RESULTS

A major objective of this study was to measure the rate of VLCFA movement across the lipid bilayer in model membranes, or the upper limit thereof, and to test whether these results are relevant to living cells. The most direct measurement of flip-flop across membranes is made by using the pH-sensitive probes pyranine or BCECF. Since FA are 50% ionized in membranes, intravesicular or intracellular acidification results from the release of $H^+$ associated with the re-equilibration of unionized FA following their flip-flop from the outer to inner membrane leaflet (17). When entrapped in cells or vesicles, these probes sensitively detect the molecules moving across the membrane (17,19,20,33). The simplest protocol for adding FA to a vesicle suspension is the unbound form, which removes the slower kinetic contribution of desorption from a donor species such as albumin or a membrane bilayer (vesicle). However, this approach does not work for VLCFA such as C20:0 ($t_{1/2}$ = 187.6 ± 8.6 sec) (see Supporting Information, Fig S1a).

Because of their very low aqueous solubility, the slow dissolution of VLCFA

aggregates in solution limits the rate of the detected change in intravesicular pH. To reduce the aqueous concentration of VLCFA to below their very low solubility limit, we used vesicles as donors for the transfer of VLCFA to acceptor vesicles containing pyranine. With this protocol, single exponential decreases in pyranine fluorescence was observed for the transfer of C20:0 (from SUV, $t_{1/2}$ = 12.1 ± 1.3 sec; from LUV $t_{1/2}$ = 57.2 ± 5.1 sec) (see Supporting Information, Fig S1b). The rate was 10-fold slower with a two carbon lengthening of the VLCFA acyl chain (C22:0 from SUV; $t_{1/2}$ = 117.2 ± 6.4 sec), in agreement with trends observed for the desorption of long-chain FA (20,22). All observed rate constants ($k_{obs}$) and associated half-time ($t_{1/2}$) values for C20:0 delivered to acceptor vesicles by various methods are listed in Table 1. Although using vesicles significantly enhanced the rate of transfer by avoiding VLCFA aggregation in solution, these experiments demonstrate that the lack of novel methodologies for rapidly delivering VLCFA to membranes poses a major challenge to isolating and studying their rate of diffusion between membrane leaflets.

*Methyl-β-cyclodextrin (MβCD) as a donor and acceptor of VLCFA.* To attempt to overcome the preceding shortcomings, we developed a new protocol in which MβCD is employed as a donor with the expectation that the MβCD would release the FA much faster than a donor vesicle, into which FA partition more favorably. Clear solutions of VLCFA with 20 to 26 carbons were prepared with MβCD at concentrations suitable for sensitive fluorescence measurements (see Methods). With MβCD as a donor for C20:0, we detected a more rapid decrease ($t_{1/2}$ < 5 sec) in the internal pH of acceptor vesicles made of PC (Fig. 1a) than when SUV were used as the donor, as shown in Table 1. Furthermore, as typically observed for uncomplexed long-chain FA (20,22), the transfer of C20:0 from MβCD was dose-dependent (Fig. 1b) within the range of C20:0/MβCD concentrations used (0.8-3 mol% C20:0 with respect to PC). . It is also important to note that these kinetics, which represent the combined steps of C20:0 dissociation from MβCD and the subsequent rate of transmembrane movement (flip-flop), were independent of the concentration of VLCFA added to the SUV.

The reversibility of the VLCFA transmembrane transport was then investigated using experimental conditions in which FA-free MβCD was employed to extract added VLCFA from vesicles made of PC (Fig. 1c). The observation of a pH increase means that VLCFA which dissociate from the outer leaflet of the membrane to bind to MβCD are rapidly replaced by un-ionized VLCFA moving from the inner leaflet in response to the changing concentration gradient across the membrane (17). As the flip-flop model predicts (17), the reverse movement of these VLCFA results in the removal of $H^+$ from the intravesicular volume to replenish the un-ionized VLCFA at the inner leaflet. We found that the time required for extraction of the C20:0, which includes both the outward flip-flop and desorption from the membrane, are faster than 5 sec. Interestingly, the concentration of MβCD required to extract C20:0 was much higher (~ 50-fold) than that required to deliver C20:0. Similar trends were also reported previously for complete extraction of oleic acid (C18:1) from vesicles under the same experimental conditions. For oleate, the concentration of MβCD is also higher than that required for delivery, but much lower than that required for the C20:0 (34), thus further reflecting the more favorable partitioning of VLCFA into membranes.

The above results for C20:0 in Fig. 1a & 1b obtained using pyranine entrapped in acceptor vesicles reflect the combined kinetic steps of: (i) dissociation of the VLCFA from various donors; (ii) adsorption of the VLCFA into the outer leaflet of the vesicle, and (iii) flip-flop across the bilayer, the last step which is directly detected by pyranine. To study the VLCFA more systematically and to make a separate measurement of adsorption, we used

acceptor vesicles (SUV and LUV) labeled with the probe FPE in the outer leaflet and containing entrapped pyranine. FPE is a fluorescein-labeled phosphatidylethanolamine phospholipid which responds to changes in membrane surface potential that occur with the binding of charged particles at the membrane surface (20,26). For C20:0 delivered from MβCD, we observed a rapid decrease in FPE fluorescence ($t_{1/2} < 5$ sec) induced by the binding of negatively-charged VLCFA anions (Fig. 2a) and a simultaneous rapid decrease ($t_{1/2} < 5$ sec) in pH, as detected by entrapped pyranine in the same vesicles (Fig. 2b). Similar results were also obtained for 22:0, 24:0, and 26:0 in PC vesicles (*data not shown*) as well as for C26:0 in FPE-labeled model raft membranes (see Fig. 3). Furthermore, we found no differences in the kinetics for either probe in both LUV and SUV acceptor vesicles (within the detection limit of our measurements), suggesting that membrane curvature of the acceptor vesicle does not play a significant role in the movement of VLCFA across the bilayer by diffusion.

*Dependence of VLCFA kinetics on temperature and media viscosity.* To assess the thermodynamic factors contributing to the activation energy of VLCFA movement across the lipid bilayer, we monitored delivery of C20:0 from MβCD to LUV at different temperatures (15-45$^{o}$C). We found no significant change in the rate within this temperature range (see Supporting Information, Fig. S2a), indicating (within the detection limit) that there is a negligible energy barrier in the process of VLCFA transport across the bilayer membrane.

Lastly, we measured the kinetics of C20:0 transfer to vesicles from MβCD while increasing the media viscosity by adding glycerol to the buffer. We observed no significant change in the kinetics of C20:0 transfer within this range of viscosities (see Supporting Information, Fig. S2b).

*VLCFA transport across and extraction from raft model lipid membranes and HEK cells*. Because of the greater hydrophobicity of VLCFA, they may better partition into ordered domains in biological membranes such as "rafts", where their biophysical transport could be altered. For comparison with the results obtained with vesicles composed only of PC, which consist of lipid bilayer in the liquid-crystalline state, we carried out additional studies for C20:0 and C26:0 to investigate bi-directional transfer between MβCD and raft model membranes (35-37) composed of an equimolar mixture of PC, cholesterol and sphingomyelin (SM). These membranes have been shown to contain both liquid-ordered and liquid-disordered lipid phases (28,38-41). The fluorescent probe Prodan, which partitions preferentially into liquid ordered phases (28), was used verify that we achieved a liquid-ordered phase in our preparation. The emission spectrum of Prodan underwent a blue shift of 60 nm (Fig. 3a), and the maximal intensity increased in the heterogeneous lipid raft model compared to the non-raft model, which is expected for the partition of Prodan into more hydrophobic region of the membrane (28).

To detect binding of the C26:0 to the outer leaflet of the bilayer of these raft model vesicles, we used FPE-labeled vesicles containing entrapped pyranine, as done for C20:0 in Fig. 2. Our results showed fast binding of C26:0 ($t_{1/2} < 5$ sec) to the raft model membrane using FPE (Fig. 3b) and equally fast transmembrane movement as detected by entrapped pyranine (Fig. 3c). Thus, the ordered domain did not result in slower adsorption of VLCFA into the outer lipid leaflet, or slower flip-flop. Because of the particular relevance of C26:0 to neurological diseases (42-44), we investigated the extraction of this VLCFA as well as C20:0 in greater depth in both PC and raft model membranes. In addition to MβCD, we also studied the extraction of hydroxypropyl beta-cyclodextrin (HPβCD) to extract these VLCFA since it is considered to be more efficient and less toxic in clinical applications of cholesterol extraction (see Discussion) (45-49). Upon addition to raft SUV (PC/SM/cholesterol

ratio = 1:1:1), C20:0 underwent rapid transfer from MβCD to the raft vesicles and then rapid desorption to bind to an excess of FA-free MβCD subsequently added to the suspension (Fig. 4a). A high (4 mM) concentration of MβCD was required to extract most of the C20:0, as in the case for its extraction from PC vesicles (Fig. 1c). However, a much higher concentration of HPβCD was required to extract the same amount of C20:0 (as measured by the increase in pyranine fluorescence) under similar experimental conditions (Fig. 4b). In parallel experiments, we observed rapid transfer and flip-flop of C26:0 (as in Fig. 3), but its extraction was measurably slower ($t_{1/2}$ = 24.5 ± 2.1 sec) than that for C20:0 ($t_{1/2}$ < 10 sec). Subsequently, we conducted experiments with vesicles composed of PC and SM, but without cholesterol (Fig. 4c inset), as well as vesicles composed of only PC (*data not shown*) to further investigate i) the effect of the model membrane structure and ii) to eliminate the possible complication of cholesterol extraction from our raft model membranes by the high MβCD concentrations added to extract C26:0 from the membrane. These comparative data indicate that enough cholesterol remained in the model raft bilayer to maintain an ordered phase that decreased the rate of extraction of C26:0. We also compared the ability of HPβCD to extract C26:0 from the raft SUV and found that a very high concentration of HPβCD (> 22 mM) extracted very little C26:0, whereas MβCD (13 mM) extracted a large proportion of the C26:0 (Fig. 4d). As a control experiment, an equivalent amount of HPβCD (FA-free) was added to a suspension of vesicles before adding the C26:0, and a small pH increase was observed as traces of FA were removed from the membrane.

To test the biological relevance of our raft model system and to examine the effects of more complex biological membranes on the transmembrane movement of VLCFA, we added C26:0/MβCD complex to a suspension of HEK cells containing the pH probe BCECF. We have previously used HEK cells to study long-chain fatty acid binding and flip-flop in part because the metabolism of the fatty acid is very slow, allowing transport processes to be observed (31,32). As with model membrane and model raft lipid vesicles, we observed a rapid decrease in BCECF fluorescence ($t_{1/2}$ < 5 sec) induced by the arrival of VLCFA at the cytosolic membrane leaflet (Fig. 5a). A rapid rise in fluorescence was observed (within seconds) with the subsequent addition of MβCD (Fig. 5b), indicating the extraction of unesterified VLCFA and consistent with the expected slow rate of VLCFA metabolism. Parallel cell imaging studies confirm a loss of FPE fluorescence at the outer membrane as C26:0 binds to the cell surface (see Supporting Information, Fig. S3) and a decrease of entrapped BCECF fluorescence after a 3 min incubation with C26:0 delivered using MβCD (Fig. 5c,d).

## DISCUSSION

In humans, the abundance of saturated FA decreases precipitously after a chain length of 18 carbons is reached. For example, glycerophospholipids in the normal brain contain 100 times more C18:0 than C20:0 (50). It is well established that VLCFA are required for membrane structure, and their content in sphingolipids is higher than in other glycerophospholipids, but when their overall levels increase in a membrane, their effects become deleterious (50). Elevated levels of VLCFA, both esterified and unesterified, in plasma and in neural tissues are markers for peroxisomal diseases including ALD. However, it is not yet clear whether these FA are causative agents. The extremely low aqueous solubility of the VLCFA has hampered their study in biophysical and physiological experiments.

This study reports new findings regarding the biophysics of VLCFA membrane transport that have potential relevance to mechanisms and therapies for neurological diseases marked by the accumulation of VLCFA. First, we used MβCD as a tool to

solubilize VLCFA to provide a new means of rapidly delivering VLCFA to the membrane surface in order to facilitate studies of their translocation across the lipid bilayer of a protein-free model membrane. Using this approach, we showed rapid ($t_{1/2} < 5$ sec) transfer of VLCFA from soluble VLCFA/MβCD complexes to vesicles. The surface probe FPE detected adsorption of the VLCFA into the outer monolayer of vesicles, and the entrapped pH dye pyranine, the flip-flop of VLCFA to the inner monolayer. These events occurred simultaneously within the time resolution of the online fluorescence experiment (Fig. 2 & 3), consistent with previous findings for long chain FA (19,20). Interestingly, membrane curvature did not have a measurable effect on these processes in the case of VLCFA.

The novel results obtained with our strategies provide the first conclusive evidence that VLCFA (20-26 carbons) diffuse rapidly across a phospholipid bilayer (liquid crystalline matrix and in a mixed phospholipid raft model matrix) without the requirement for a protein transporter. The results with the raft model membranes and HEK cells validate the data obtained in simple model membranes and suggest that VLCFA will diffuse rapidly in biological membranes, even in the presence of more ordered membrane domains. With this new knowledge, it is unlikely that a protein such as the ALDP is required to transport VLCFA across peroxisomal membranes, and reasons for VLCFA accumulation are not likely due to disregulated transmembrane transport by a protein. Other mechanisms, including disregulated transport and/or metabolism of the membrane impermeable acyl-CoA (51), now appear more plausible and worthy of investigation.

The second new finding, the extraction of VLCFA, especially C26:0, from lipid membranes by MβCD, may provide a new therapeutic approach. In the case of C26:0, the previously reported $t_{1/2}$ of dissociation from model membranes to acceptors (vesicle and albumin) is four orders of magnitude slower than that for dietary 18-carbon FA (24). This led us to hypothesize that the longevity of the VLCFA in a membrane would enhance its deleterious effects, and make it more difficult to remove from the site(s) where it exerts these effects. The present study shows that VLCFA are rapidly extracted ($t_{1/2}$ of seconds) by excess MβCD, representing a several-fold improvement in natural membrane dissociation rate for VLCFA such as C26:0. In another study with dietary fatty acids (oleic acid; C18:1), high concentrations of MβCD also extracted these FA from vesicles (52) but with a rate comparable to the known faster rates of their dissociation from membrane (22,24), thus offering no further enhancement of extraction rates.

The result for C26:0 is not altogether unexpected, since cholesterol is also extracted from membranes on the same time scale (53). In model membranes (without adding MβCD), cholesterol and C26:0 have the same hydrophobicity and the same slow rate of dissociation. Moreover, the concentration of MβCD needed to extract most or all of the C26:0 in our model membranes was comparable to the concentration used to extract cholesterol from cell membranes (mM).

Most therapeutic approaches for the treatment of ALD/AMN patients thus far have focused on preventing the accumulation of VLCFA, either by imposing dietary restrictions or addition of Lorenzo's Oil to the diet (54-57). These therapies are more successful in lowering plasma levels of VLCFA than in lowering levels of VLCFA in the brain. Currently, there are no tools for extracting the abnormal levels of unesterifed VLCFA which have already accumulated in membranes. Our new findings showing that MβCD can rapidly extract VLCFA from phospholipid bilayers and cell membranes suggest that a more effective therapy could come from new methods that focus on reducing the concentration of unesterified VLCFA in the plasma and in plasma membranes of cells in contact with the circulation system.

Interestingly, cyclodextrins have recently been reported to correct NPC1-null mouse models of disease, Niemann-Pick type C, a neurodegenerative disorder characterized by greatly altered somatic cholesterol metabolism (45,58). Treatment with hydroxypropyl-β-cyclodextrins (HPβCD), delayed neurological symptoms and decreased cholesterol storage in the liver. Very recently, pilot tests in children with Niemann-Pick C disease began after FDA approval of HPβCD for this purpose. We compared the ability of MβCD and HPβCD for extraction of C26:0 from our model membranes and found that MβCD was much more effective for C26:0, although both cyclodextrins effectively extracted C20:0 from membranes (Fig. 4). Since HPβCD is considered to be less toxic for these types of treatments, further studies of the effectiveness of different cyclodextrins are needed. We have initiated collaborative studies of the effect of excess VLCFA (intravenous infusion as a MβCD complex) on demyelination in a mouse model. These studies will then be extended to test the reversibility with the infusion of FA-free cyclodextrins.

We thank Florian Eichler for many helpful comments.

This work was supported by funding from the NIH (Grant No. HL26335)

## REFERENCES

1. Moser, H. W., and Moser, A. B. (1996) *Lipids* **31 Suppl**, S141-144
2. Eichler, F. S., Ren, J. Q., Cossoy, M., Rietsch, A. M., Nagpal, S., Moser, A. B., Frosch, M. P., and Ransohoff, R. M. (2008) *Ann Neurol* **63**, 729-742
3. Grkovic, S., Dordevic, M., Nikolic, R., Zivancevic-Simonovic, S., and Puzigaca, Z. (2007) *Med Pregl* **60**, 401-403
4. Hein, S., Schonfeld, P., Kahlert, S., and Reiser, G. (2008) *Hum Mol Genet* **17**, 1750-1761
5. Heinzer, A. K., Watkins, P. A., Lu, J. F., Kemp, S., Moser, A. B., Li, Y. Y., Mihalik, S., Powers, J. M., and Smith, K. D. (2003) *Hum Mol Genet* **12**, 1145-1154
6. Steinberg, S., Jones, R., Tiffany, C., and Moser, A. (2008) *Curr Protoc Hum Genet* **Chapter 17**, Unit 17 16
7. Poggi-Travert, F., Fournier, B., Poll-The, B. T., and Saudubray, J. M. (1995) *J Inherit Metab Dis* **18 Suppl 1**, 1-18
8. Singh, H., Derwas, N., and Poulos, A. (1987) *Arch Biochem Biophys* **257**, 302-314
9. Singh, H., Derwas, N., and Poulos, A. (1987) *Arch Biochem Biophys* **259**, 382-390
10. Singh, H., Derwas, N., and Poulos, A. (1987) *Arch Biochem Biophys* **254**, 526-533
11. van Roermund, C. W., Visser, W. F., Ijlst, L., van Cruchten, A., Boek, M., Kulik, W., Waterham, H. R., and Wanders, R. J. (2008) *FASEB J* **22**, 4201-4208
12. Kemp, S., Valianpour, F., Denis, S., Ofman, R., Sanders, R. J., Mooyer, P., Barth, P. G., and Wanders, R. J. (2005) *Mol Genet Metab* **84**, 144-151
13. Corzo, D., Gibson, W., Johnson, K., Mitchell, G., LePage, G., Cox, G. F., Casey, R., Zeiss, C., Tyson, H., Cutting, G. R., Raymond, G. V., Smith, K. D., Watkins,

P. A., Moser, A. B., Moser, H. W., and Steinberg, S. J. (2002) *Am J Hum Genet* **70**, 1520-1531
14. Cartier, N., Lopez, J., Moullier, P., Rocchiccioli, F., Rolland, M. O., Jorge, P., Mosser, J., Mandel, J. L., Bougneres, P. F., Danos, O., and et al. (1995) *Proc Natl Acad Sci U S A* **92**, 1674-1678
15. Hettema, E. H., and Tabak, H. F. (2000) *Biochim Biophys Acta* **1486**, 18-27
16. Kamp, F., Guo, W., Souto, R., Pilch, P. F., Corkey, B. E., and Hamilton, J. A. (2003) *J Biol Chem* **278**, 7988-7995
17. Kamp, F., and Hamilton, J. A. (1992) *Proc Natl Acad Sci U S A* **89**, 11367-11370
18. Kleinfeld, A. M., Chu, P., and Romero, C. (1997) *Biochemistry* **36**, 14146-14158
19. Simard, J. R., Kamp, F., and Hamilton, J. A. (2008) *Biophys J* **94**, 4493-4503
20. Simard, J. R., Pillai, B. K., and Hamilton, J. A. (2008) *Biochemistry* **47**, 9081-9089
21. Veerkamp, J. H., and Maatman, R. G. (1995) *Prog Lipid Res* **34**, 17-52
22. Zhang, F., Kamp, F., and Hamilton, J. A. (1996) *Biochemistry* **35**, 16055-16060
23. Choi, J. K., Ho, J., Curry, S., Qin, D., Bittman, R., and Hamilton, J. A. (2002) *J Lipid Res* **43**, 1000-1010
24. Ho, J. K., Moser, H., Kishimoto, Y., and Hamilton, J. A. (1995) *J Clin Invest* **96**, 1455-1463
25. Orosz, D. E., and Garlid, K. D. (1993) *Anal Biochem* **210**, 7-15
26. Wall, J., Golding, C. A., Van Veen, M., and O'Shea, P. (1995) *Mol Membr Biol* **12**, 183-192
27. Asawakarn, T., Cladera, J., and O'Shea, P. (2001) *J Biol Chem* **276**, 38457-38463
28. Bondar, O. P., and Rowe, E. S. (1999) *Biophys J* **76**, 956-962
29. Macgregor, R. B., and Weber, G. (1986) *Nature* **319**, 70-73
30. Weber, G., and Farris, F. J. (1979) *Biochemistry* **18**, 3075-3078
31. Meshulam, T., Simard, J. R., Wharton, J., Hamilton, J. A., and Pilch, P. F. (2006) *Biochemistry* **45**, 2882-2893
32. Simard, J. R., Meshulam, T., Pillai, B. K., Kirber, M. T., Brunaldi, K., Xu, S., Pilch, P. F., and Hamilton, J. A. (2009) *J Lipid Res*
33. Kamp, F., Zakim, D., Zhang, F., Noy, N., and Hamilton, J. A. (1995) *Biochemistry* **34**, 11928-11937
34. Hamilton, J. A., and Brunaldi, K. (2007) *J Mol Neurosci* **33**, 12-17
35. Dietrich, C., Bagatolli, L. A., Volovyk, Z. N., Thompson, N. L., Levi, M., Jacobson, K., and Gratton, E. (2001) *Biophys J* **80**, 1417-1428
36. Putzel, G. G., and Schick, M. (2009) *Biophys J* **96**, 4935-4940
37. Rawicz, W., Smith, B. A., McIntosh, T. J., Simon, S. A., and Evans, E. (2008) *Biophys J* **94**, 4725-4736
38. Krasnowska, E. K., Bagatolli, L. A., Gratton, E., and Parasassi, T. (2001) *Biochim Biophys Acta* **1511**, 330-340
39. Krasnowska, E. K., Gratton, E., and Parasassi, T. (1998) *Biophys J* **74**, 1984-1993
40. Massey, J. B., She, H. S., and Pownall, H. J. (1985) *Biochemistry* **24**, 6973-6978
41. Tamai, N., Uemura, M., Goto, M., Matsuki, H., and Kaneshina, S. (2008) *Colloids Surf B Biointerfaces* **65**, 213-219

42. Deon, M., Garcia, M. P., Sitta, A., Barschak, A. G., Coelho, D. M., Schimit, G. O., Pigatto, M., Jardim, L. B., Wajner, M., Giugliani, R., and Vargas, C. R. (2008) *Metab Brain Dis* **23**, 43-49
43. Di Biase, A., Avellino, C., Pieroni, F., Quaresima, T., Grisolia, A., Cappa, M., and Salvati, S. (1997) *Neurochem Res* **22**, 327-331
44. Whitcomb, R. W., Linehan, W. M., and Knazek, R. A. (1988) *J Clin Invest* **81**, 185-188
45. Camargo, F., Erickson, R. P., Garver, W. S., Hossain, G. S., Carbone, P. N., Heidenreich, R. A., and Blanchard, J. (2001) *Life Sci* **70**, 131-142
46. Kilsdonk, E. P., Yancey, P. G., Stoudt, G. W., Bangerter, F. W., Johnson, W. J., Phillips, M. C., and Rothblat, G. H. (1995) *J Biol Chem* **270**, 17250-17256
47. Kritharides, L., Kus, M., Brown, A. J., Jessup, W., and Dean, R. T. (1996) *J Biol Chem* **271**, 27450-27455
48. Rawyler, A., and Siegenthaler, P. A. (1996) *Biochim Biophys Acta* **1278**, 89-97
49. Yancey, P. G., Rodrigueza, W. V., Kilsdonk, E. P., Stoudt, G. W., Johnson, W. J., Phillips, M. C., and Rothblat, G. H. (1996) *J Biol Chem* **271**, 16026-16034
50. Theda, C., Moser, A. B., Powers, J. M., and Moser, H. W. (1992) *J Neurol Sci* **110**, 195-204
51. Boylan, J. G., and Hamilton, J. A. (1992) *Biochemistry* **31**, 557-567
52. Brunaldi, K., Huang, N., and Hamilton, J. A. (2009) *J Lipid Res*
53. Hamilton, J. A. (2003) *Curr Opin Lipidol* **14**, 263-271
54. Moser, H. W. (1995) *J Neuropathol Exp Neurol* **54**, 740-745
55. Moser, H. W., and Borel, J. (1995) *Annu Rev Nutr* **15**, 379-397
56. Moser, H. W., Moser, A. B., Hollandsworth, K., Brereton, N. H., and Raymond, G. V. (2007) *J Mol Neurosci* **33**, 105-113
57. van Geel, B. M., Assies, J., Haverkort, E. B., Koelman, J. H., Verbeeten, B., Jr., Wanders, R. J., and Barth, P. G. (1999) *J Neurol Neurosurg Psychiatry* **67**, 290-299
58. Liu, B., Turley, S. D., Burns, D. K., Miller, A. M., Repa, J. J., and Dietschy, J. M. (2009) *Proc Natl Acad Sci U S A* **106**, 2377-2382
59. Covey, S. D., Brunet, R. H., Gandhi, S. G., McFarlane, N., Boreham, D. R., Gerber, G. E., and Trigatti, B. L. (2007) *Biochem Biophys Res Commun* **355**, 67-71
60. Frank, P. G., Marcel, Y. L., Connelly, M. A., Lublin, D. M., Franklin, V., Williams, D. L., and Lisanti, M. P. (2002) *Biochemistry* **41**, 11931-11940
61. Klymchenko, A. S., Duportail, G., Demchenko, A. P., and Mely, Y. (2004) *Biophys J* **86**, 2929-2941
62. Wilson-Ashworth, H. A., Bahm, Q., Erickson, J., Shinkle, A., Vu, M. P., Woodbury, D., and Bell, J. D. (2006) *Biophys J* **91**, 4091-4101

## FOOTNOTES

*This work is supported in part by Grant NIH-NHLBI 2P01 HL26335-21.

The abbreviations are: FA, fatty acid; VLCFA, very long chain fatty acid, AMN, adrenomyeloneuropathy; ALD, adrenoleukodystrophy; PC, phosphatidylcholine, MβCD, methyl-beta-cyclodextrin; HPβCD, hydroxypropyl-beta-cyclodextrin; ALDP, adrenoleukodystropy protein; VLACS, very long chain acyl CoA synthetase activity; SM, sphingomyelin; FPE; fluorescein-phosphatidylethanolamine

## KEYWORDS

VLCFA, lipid raft, transport, membrane, FPE, peroxisomal disorders

## FIGURE LEGENDS

Fig. 1. Binding and extraction of arachidic acid (C20:0) from SUV/LUV containing pyranine. **A.** Addition of C20:0 complexed to donor SUV (12 mol% relative to PC) results in the slow arrival ($t_{1/2}$ ~11 sec) of these VLCFA at the inner membrane leaflet of acceptor vesicles. *Note: Vesicle and acceptor donors were mixed in a 1:1 ratio such that the net transfer of VLCFA was ~ 6 mole% to the acceptor vesicles.* Delivery of C20:0 complexed to MβCD (6 mole% relative to PC) was much faster ($t_{1/2}$ < 5 sec), suggesting that the slow transfer of C20:0 from SUV is the result of its slow desorption from the donor membrane. The fluorescence trace of C20:0 transfer from donor to acceptor SUV was fitted as a single exponential function to obtain the kinetic rate constant ($k_{obs}$) or half-time of fluorescence decay ($t_{1/2}$). MβCD effectively increases C20:0 solubility, enhances rapid delivery to the outer membrane, allowing the fast flip-flop of VLCFA to the inner leaflet to be monitored independent of slower kinetic steps. The magnitude of pH drop was the same in both experiments, indicating that an equal amount of C20:0 was delivered to the acceptor membrane. **B.** The transfer of C20:0 from MβCD (0.8-3 mole% relative to PC) to acceptor SUV is dose-dependant. The addition of increasing amounts of C20:0 complexed with MβCD resulted in larger pH decreases as predicted by the flip-flop model (17). **C.** Extraction of C20:0 from pre-loaded LUV (6 mol% relative to PC) by MβCD. The addition of MβCD causes (black arrow) C20:0 to leave the LUV, resulting in an increase in pyranine fluorescence, as expected (17). Different concentrations of MβCD (1.2, 2.5, 5 mM) resulted in a dose-dependent fluorescence increase. It is interesting to note that the concentrations of MβCD required to extract C20:0 from membranes under these conditions (~5-7 mM) was similar to concentration classically employed to extract cholesterol from membranes (59,60). All traces shown are representative traces from at least 3 independent experiments.

Fig. 2. Binding and transmembrane movement of arachidic acid (C20:0) across the membrane bilayer of LUV, **A.** Partitioning of C20:0 (6 mole% relative to PC) to LUV was detected using surface potential probe FPE. Addition of a single dose of C20:0

complexed to MβCD to acceptor LUV labeled with FPE results in fast decrease in FPE fluorescence ($t_{1/2}$ < 5 sec) as the VLCFA bind quickly to the outer membrane leaflet. **B.** The flip-flop of C20:0 to the inner membrane leaflet was accomplished by using entrapped pyranine. The addition of C20:0 (6 mole% relative to PC) also resulted in a rapid decrease in pyranine fluorescence ($t_{1/2}$ < 5 sec). Since our dual-fluorescence approach reports on events simultaneously at each side of the membrane, our results clearly demonstrate the rapid flip-flop of VLCFA in LUV, which have a lower surface curvature than SUV and more closely model the curvature of the plasma membrane. All traces shown are representative traces from at least 3 independent experiments.

Fig. 3. Flip-flop of hexacosanoic acid (C26:0) in a raft model lipid membrane. Model raft membranes were prepared using PC, sphingomyelin and cholesterol (mixed 1:1:1) and labeled with surface potential probe FPE on the outer membrane and containing the pH sensitive dye pyranine. Prodan is an environmentally-sensitive probe (30,61,62) and was used to differentiate raft model membranes from the non-raft regions of membrane. **A.** As expected, the emission spectra of the Prodan shows a large blue shift in the lipid raft model compared to the non-raft PC bilayer. B. Addition of C26:0/MβCD complex (6 mole% relative to PC) to the acceptor raft model SUV labeled with FPE showed that C26:0 binds rapidly to the outer membrane leaflet. **C.** The response of entrapped pyranine indicated rapid flip-flop of C26:0 (6 mole% relative to PC) to the inner leaflet. These measurements demonstrate that VLCFA diffuse across more complex and rigid protein-free model membranes with a $t_{1/2}$ < 5 sec. All traces shown are representative traces from at least 3 independent experiments.

Fig.4. Bi-directional studies of the transmembrane movement of arachidic acid (C20:0) and hexacosanoic acid (C26:0) across the membrane bilayer. **A.** Upon addition of C20:0/MβCD complex (6 mole% relative to PC) to raft SUV, fast flip-flop was observed ($t_{1/2}$ < 5 sec) similar to that observed in non-raft model vesicles (see Fig. 3). The subsequent addition of 4 mM MβCD rapidly extracts C20:0 from the raft model membranes ($t_{1/2}$ < 10 sec) **B.** More than 8-fold higher amounts of HPβCD were required to extract a similar concentration of C20:0. **C.** In parallel experiments, the addition of C26:0 (6 mole% relative to PC) also showed a fast flip-flop ($t_{1/2}$ < 5 sec) across raft model membranes, but the extraction of C26:0 from the raft membrane was much slower ($t_{1/2}$ ~ 25 sec) when compared to the rate of extraction of C26:0 from membranes which do not contain cholesterol (inset). **D.** After addition of a similar amount of C26:0, HPβCD concentrations up to 22 mM rapidly extracted only small amounts of C26:0 from the raft SUV (inset) while 13 mM MβCD extracted a significant proportion of C26:0. *Note: Prior to the addition of C26:0 complexed with MβCD, traces of long chain FA present in the raft SUV were removed by ~2 mM of MβCD.*

Fig. 5. Transmembrane movement of VLCFA into HEK cells. Plated HEK293 cells were suspended in buffer prior to real-time fluorescence measurements in a rapidly-stirred cuvette. A**.** The flip-flop of C26:0 to the cytosolic leaflet of HEK cells was accomplished by using entrapped BCECF. The addition of C26:0/MβCD complex (20 μM) resulted in a rapid decrease in BCECF fluorescence ($t_{1/2}$ < 5 sec). The trace shown is representative of the traces obtained from at least 3 independent experiments. **B.** The flip-

flop of C26:0 (delivered as 15 μM C26:0/MβCD complex) was detected by using entrapped BCECF. C26:0 was then rapidly extracted from HEK cells with excess FA-free MβCD. The trace shown is representative of the traces obtained from at least 3 independent experiments. **C.** Image of single HEK cells loaded with BCECF. BCECF was clearly confined to the cytosol. **D.** Image captured after the addition of C26:0 delivered as a complex with MβCD (30 μM). Images show a decrease in BCECF intensity after 3 min incubation, indicating that C26:0 was delivered to the cell surface by MβCD, reached the cytosolic leaflet and acidified the cytosol. Note that due to the inability to rapidly mix VLCFA with cells under these conditions, single cell measurements do not allow accurate measurement of the kinetics of transmembrane movement. Furthermore, using 30 μM MβCD to deliver VLCFA was not accompanied by any detectable changes in cell membrane morphology. Control experiments with addition of an equal amount of MβCD showed no decrease in fluorescence intensity.

Table 1. Desorption rate constants and $t_{1/2}$ for arachidic acid (C20:0) from different donors. In all experiments, approximately 6 mole% C20:0 was transferred to the acceptor vesicles. The observed rate constant ($k_{obs}$) of the fluorescence change was obtained by fitting the fluorescence trace to the first order decay function. All reported values are the mean +/- s.d. of at least 3 independent measurements.

**Figure 1**

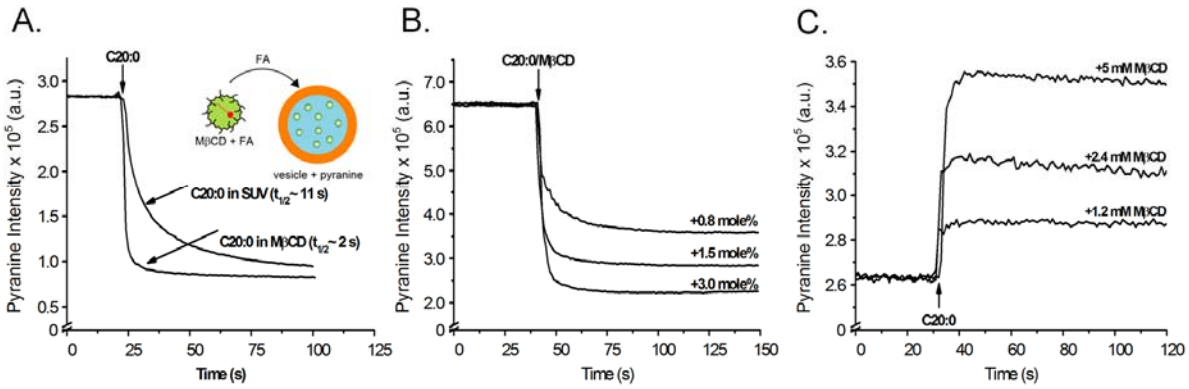

**Figure 2**

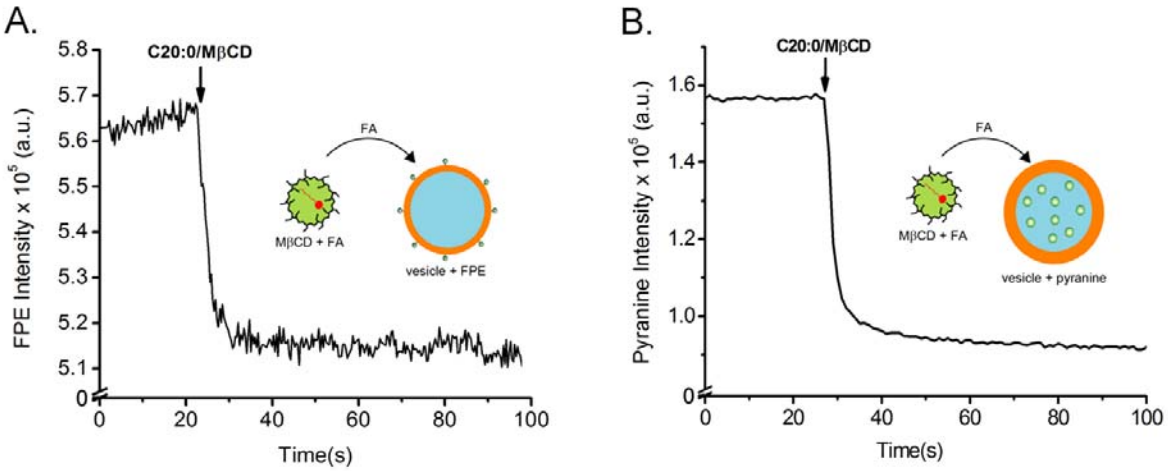

**Figure 3**

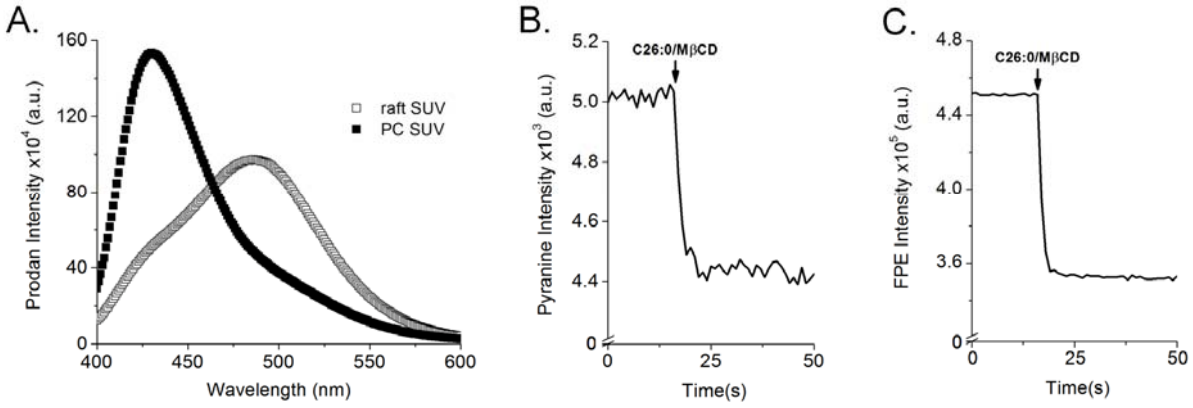

**Figure 4**

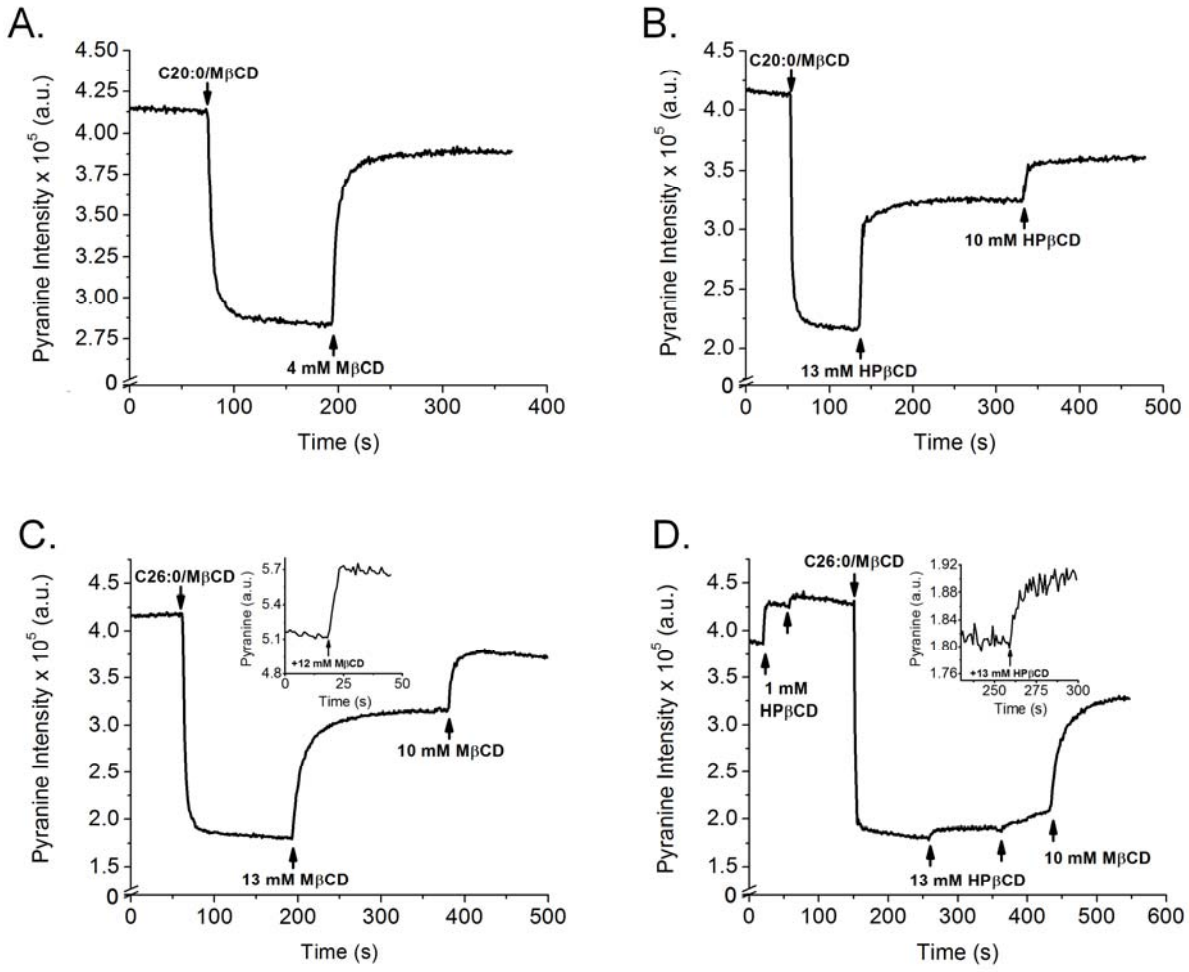

**Figure 5:**

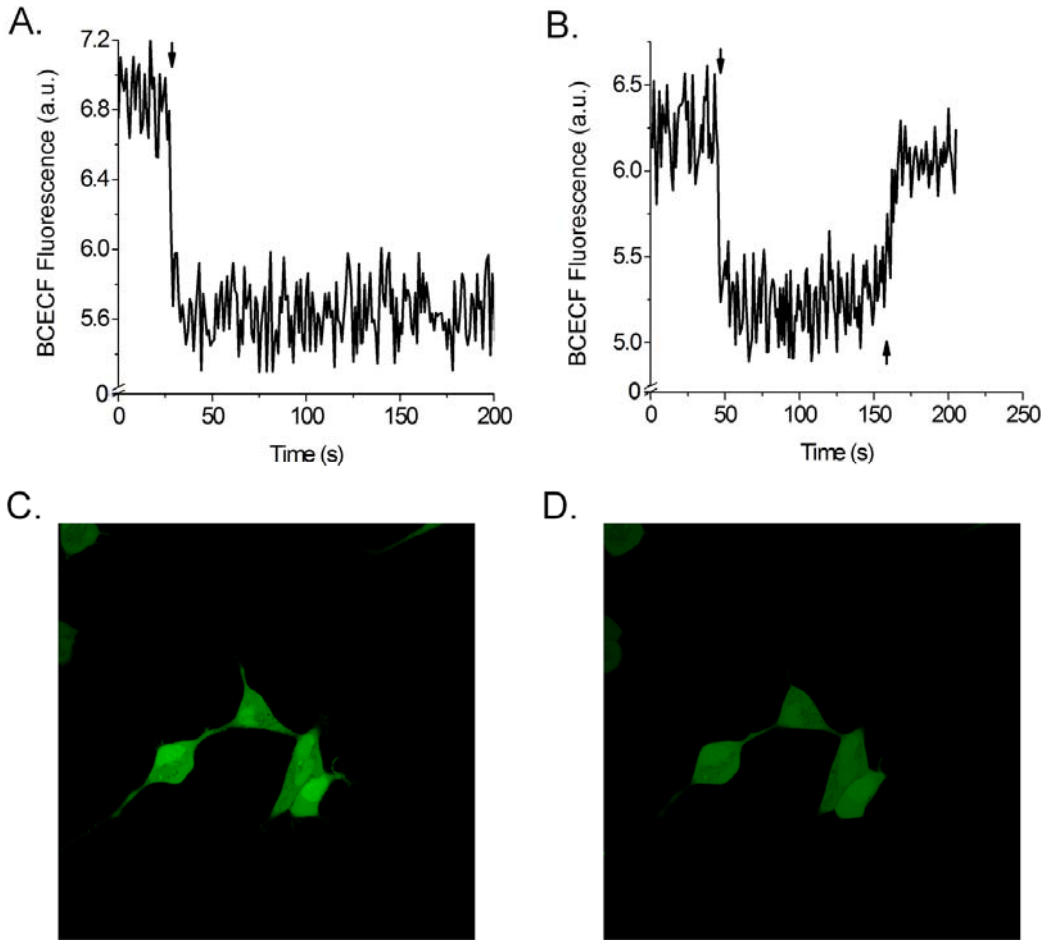

**Table 1**

| Delivery System | $k_{obs}$ ($s^{-1}$) | $t_{1/2}$ (sec) |
|---|---|---|
| **unbound FA** | 0.00370 ± 0.00017 | 187.6 ± 8.6 |
| **FA/LUV complex** | 0.0122 ± 0.0010 | 57.2 ± 5.1 |
| **FA/SUV complex** | 0.0577 ± 0.0061 | 12.1 ± 1.3 |
| **FA/CD complex to SUV** | 0.222 ± 0.056 | 3.3 ± 0.8 |
| **FA/CD complex to LUV** | 0.243 ± 0.010 | 2.9 ± 0.1 |